ELSEVIER

Thin Solid Films 337 (1999) 166–170

thin solid films

Self-assembly of ultrathin composite TiO_2/polymer films

N. Kovtyukhova[a,*], P.J. Ollivier[b], S. Chizhik[c], A. Dubravin[c], E. Buzaneva[d], A. Gorchinskiy[d], A. Marchenko[e], N. Smirnova[a]

[a]*Institute of Surface Chemistry, 31, Pr. Nauky, 252022 Kiev, Ukraine*
[b]*The Pennsylvania State University, University Park, PA 16802, USA,*
[c]*Metal-Polymer Research Institute, 32A, Kirov Str., 246652 Gomel, Byelorussia*
[d]*National T.Shevchenko University, 64, Vladimirskaya Str., 252033 Kiev, Ukraine*
[e]*Institute of Physics, 48, Pr. Nauky, 252022 Kiev, Ukraine*

Abstract

A wet layer-by-layer self-assembly of composite TiO_2/polymer films on Si and Al_2O_3/Al, substrates has been studied by AFM, STM, and ellipsometry techniques. The quality of the first adsorbed TiO_2 layer has been found to be the governing factor in multilayer film growth. The first layer consists of single particles and particle agglomerates 30–120 nm wide The surface coverage in the layer is determined by the chemical composition of the substrate surface and water pH in post-adsorption rinsing procedure. Well-packed TiO_2/polymer film completely covering the surface has been prepared in five adsorption cycle on Al_2O_3/Al substrate. The film remained crack-free after heat treatment at 300°C. *I–V* curves measurement reveals high resistivity ($R \sim 10^{10}$ O in the voltage range from −2 to +3 V) of TiO_2/polymer films prepared in ten adsorption cycles.

Keywords: Titanium oxide; Polymer; Wet layer-by-layer deposition; Surface morphology; Electrical properties

1. Introduction

Nanostructured TiO_2 films possess unique characteristics that provide a wide range of applications as transparent conductive films in solar cells [1–4], transparent ceramic membranes [5], antireflection coatings [6], insulating layers, photoelectrodes [7–9], and photocatalysts [10,11].

Fabrication of titania films with thickness control to nanometer precision is an important technology leading to wide applications in future [12]. Using electron-beam, magnetron and rf-sputtering deposition techniques, the fabrication of stoichiometric and homogeneous-thickness thin TiO_2 films was found difficult due to the possible spontaneous growth of single TiO_x islands during the initial stage of the film formation.

A wet procedure of layer by layer self-assembly of TiO_2/polymer films from titania colloidal particles and organic macromolecules, which are held together by non-specific bonding forces at a solid/solution interface, has shown its worth as a cheap and technologically very simple method for the construction of ultrathin nanostructured composite films [13,14]. Using this technique, surfaces can be permanently derivatised with films in which layers of TiO_2 nanoparticles and polymeric 'spacers' alternate along the stacking axis [13,14]. Significantly, judicious selection of components can result in nanostructured films with the desired optical, electronic, magnetic, mechanical, and thermal properties due to combining advantages of inorganic and organic precursors.

The lateral topography of the film is one of the most important factors affecting the transport properties and carrier mobilities of the complete assemblies. In many self-assembled systems, adsorption of mono- and multilayers displaying structural order has proven difficult. Understanding of the lateral/vertical organization of the component particles in the film is of crucial importance for the synthesis of new composite materials with required optical, electronic properties. This work is aimed at the direct observation (by AFM and STM techniques) of the layer-by-layer self-assembly of TiO_2/polymer composite films on conducting (Al_2O_3/Al, ITO) and non-conducting (Si) substrates, and the investigation of their electronic properties for potential applications in electronic systems.

2. Experimental

Titania solution was prepared by dissolving $Ti(ipro)_4$ in methylcellosolve in the presence of HCl to give 4% (w/w)

* Corresponding author. Fax: +380-44-2640446;
e-mail: nik@surfchem.freenet.kiev.ua.

0040-6090/99/$ - see front matter
PII S0040-6090(98)01197-3

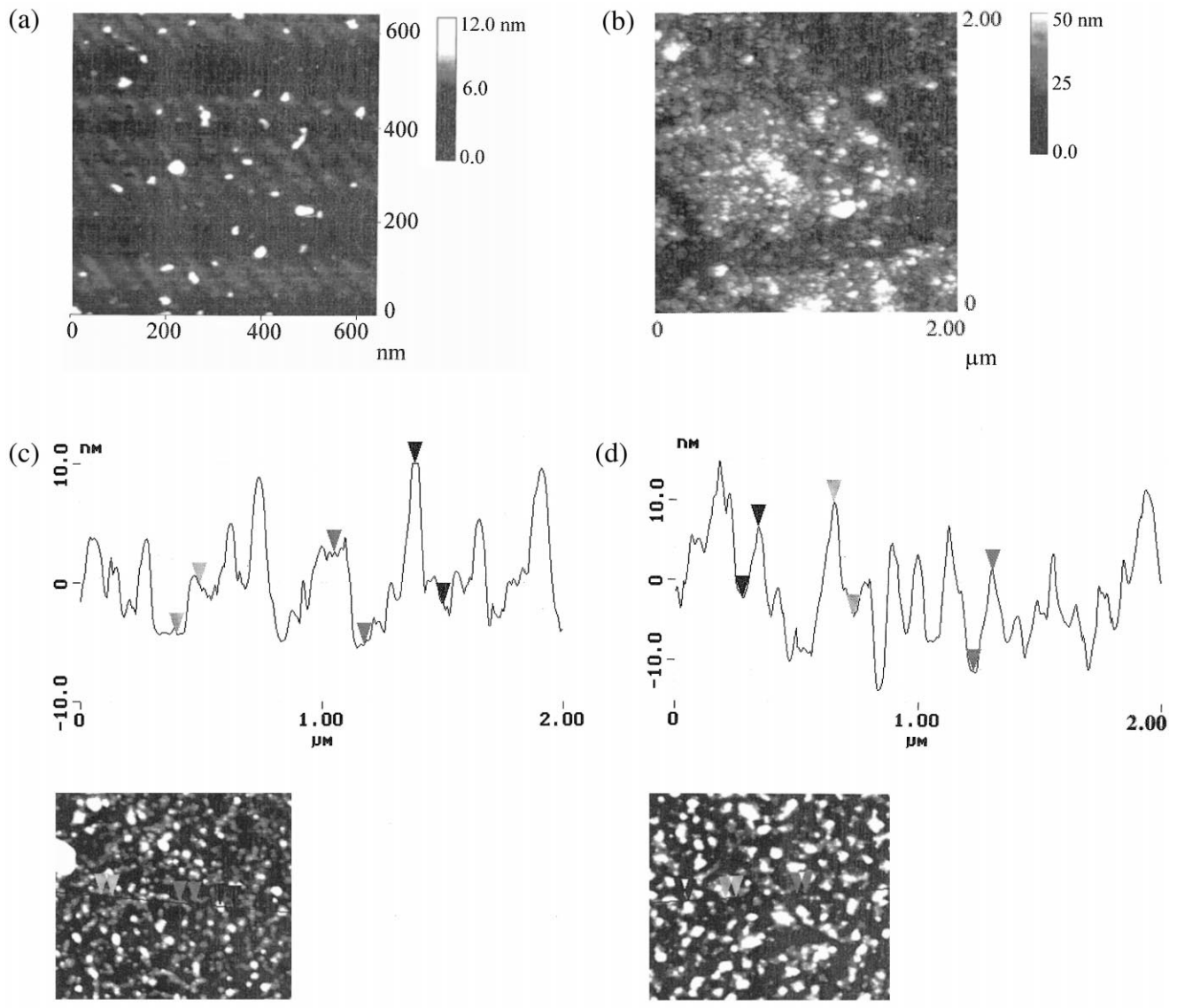

Fig. 1. Tapping-mode AFM images of the first TiO_2 layer (a,b,c) and multilayer $(TiO_2/PAH)_4TiO_2$ film (d). (a) $Si(NH_2)$ substrate, deposition procedure involved rinsing with deionised water; (b) $Si(NH_2)$ substrate, deposition procedure involved rinsing with water of pH 2; (c) Al_2O_3/Al substrate; (d) $Si(NH_2)$ substrate. Surface profile taken along the line, as shown in b and d, allows to estimate the features height, which varies in the range of 4–13 nm for the first deposited TiO_2 layer (b) and 9–14 nm for multilayer $(TiO_2/PAH)_4TiO_2$ film (d).

solution. The solution was diluted with water to adjust the concentration to 1% and allowed to age during 3 weeks. Then water was evaporated at 60°C. Resultant xerogel containing 75% (w/w) titania was used for the preparation of stable hydrosol (4.75%, pH 2) during several weeks. Aqueous solutions of poly(allylamine hydrochloride), PAH (0.01M, pH 7); polyethylenimine, PEI (0.65%, pH 9); and doped polyaniline, PAN (pH 2.5) [15] were used for film preparation.

The surface of polished Si wafers was hydroxylated by 30 min sonication in 'piranha' solution (4:1 conc.H_2SO_4/30% H_2O_2). First priming the hydroxylated silicon wafers with 4-((dimethylmethoxy)silyl)butylamine (15 h treatment with 5% toluene solution) initiated growth of the TiO_2 films. The primed Si substrate is designated in the text as $Si(NH_2)$. An aluminium foil bearing a native oxide, Al/Al_2O_3, and ITO-coated glass (Delta Technologies) were cleaned by sonicating in hexane or aqueous ethanolamine solution (20%), respectively.

For film preparations, a substrate was alternately immersed in TiO_2 solution and polymer solution for 15 min. Every immersion was followed by rinsing with deionised water and drying in an Ar stream.

AFM images.were obtained with a Digital Instruments Nanoscope IIIa in tapping mode. STM images.were obtained in air with a home-built microscope [16] in the constant current mode. Ellipsometric measurements were made with an ellipsometer from Gaertner Scientific Corp. *I–V* characteristics were measured at ambient temperature using home-constructed tunnelling spectrometer with

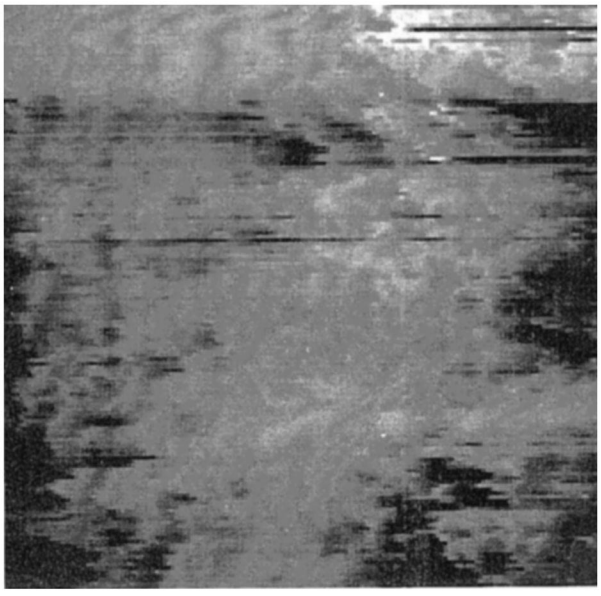

Fig. 2. STM image (600 × 600 Å) of the first TiO_2 layer deposited onto Al_2O_3/Al substrate: $V = 0.2$ eV, $I = 0.4$ nA.

permanent distance (1 mm) between Pt or Cu probes (diameter 0.01 mm).

3. Results and discussion

3.1. Characterization of the TiO_2 colloid

Transmission electron microscopy investigation (JEOL 1200 EXII) of the 4.75% TiO_2 solution reveals particles of different shape and size approximately ranging from 4 to 13 nm, though most of the particles have size of about 5–7 nm. X-Rray diffractogram (Cu Kα radiation) of the starting xerogel (is not presented) indicates a weak signal of anatase at about 26°. The average particle diameter calculated by the Scherrer equation is ~6 nm. UV-Vis spectrum (Hitachi U-3000) of the TiO_2 solution shows the blue shift of the absorption edge of the titania solution compared to bulk titania (362 vs. 388 nm) that indicates the expansion of the effective bandgap by 0.2 eV (3.4 vs. 3.2 eV). This may be caused by the fact that the valence band in small particles is not completed within their volume in contrast to bulk solids.

3.2. AFM and STM of the first deposited TiO_2 layer

AFM image of the TiO_2 layer that has been deposited in one adsorption cycle onto NH_2-terminated Si surface (Fig. 1a) shows separate features relatively evenly disposed on a distance of 30–250 nm from one another. Obviously, the features, which are approx. 12 nm high and 20– 70 nm in diameter, are agglomerates formed from several (3–15) TiO_2 particles aggregated in the horizontal plane. Surface coverage was estimated at about 25%. Using water with pH adjusted to 2, the same pH as that of the starting titania solution, instead of water (pH 7) in the post-deposition rinsing procedure results in a much closer-packed layer of the well-distinguished TiO_2 particle agglomerates (Fig. 1b). The agglomerates have a larger diameter (30–120 nm) and form islands of the film. Lateral dimensions of the islands are estimated at 250–800 nm and their height at 4–13 nm. Surface coverage is about 85%. Hence titania nanoparticles can be removed from the NH_2-terminated Si surface during post-deposition rinsing with deionised water. This indicates that at neutral pH the potentials of diffusion layers on Si(NH_2) and TiO_2 particles surfaces change and repulsion between them increases.

AFM image of the Al_2O_3/Al substrate that has been treated with one TiO_2 adsorption cycle (Fig. 1c) reveals distinct features of the different shape and size and no voidks between them that indicates the formation of monolayer film from the TiO_2 particles. The features' diameter ranges from 20 nm to 100 nm (though more extended features up to 200 nm are also observed). Taking into account that the size of TiO_2 particles in the starting solution is 4–13 nm, one can conclude that the TiO_2 film consists of agglomerates with particles number varying from units to tens.

More detailed information on the TiO_2 layer surface morphology with a length scale of about 1 nm can be obtained by STM, assuming that the single TiO_2 particles have electronic conductivity due to surface and/or internal defect states. The STM topograph of the first TiO_2 layer deposited on the Al_2O_3/Al substrate (Fig. 2) shows the parti-

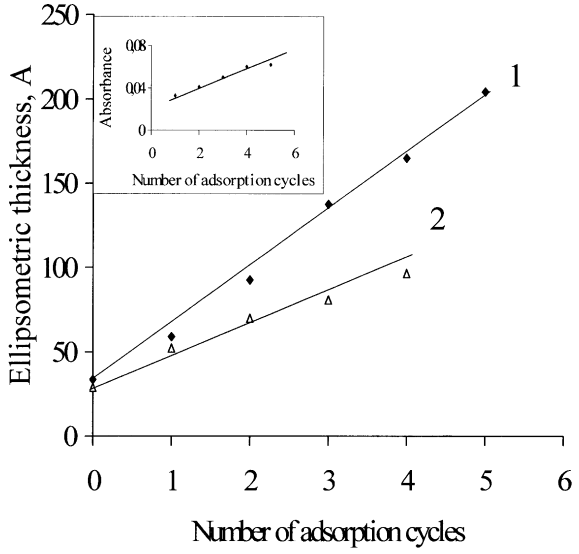

Fig. 3. Ellipsometric measurements of the thickness of multilayer TiO_2/PAH films on Si(NH_2) substrate vs. number of adsorption cycles. Analyzing wavelength: 4880 Å; Si refractive indices: $n_s = 3.875$ and $k_s = -0.018$; refractive index of TiO_2/PAH film: $n_f = 1.540$. The points on the plots refer to films terminated by a TiO_2 layer. The deposition procedure involved rinsing with: (1) deionised water (pH 7), (2) acidified water (pH 2). The absorbances at 364 nm vs. the number of the adsorption TiO_2/PEI cycles (substrate: glass) are plotted in the inset.

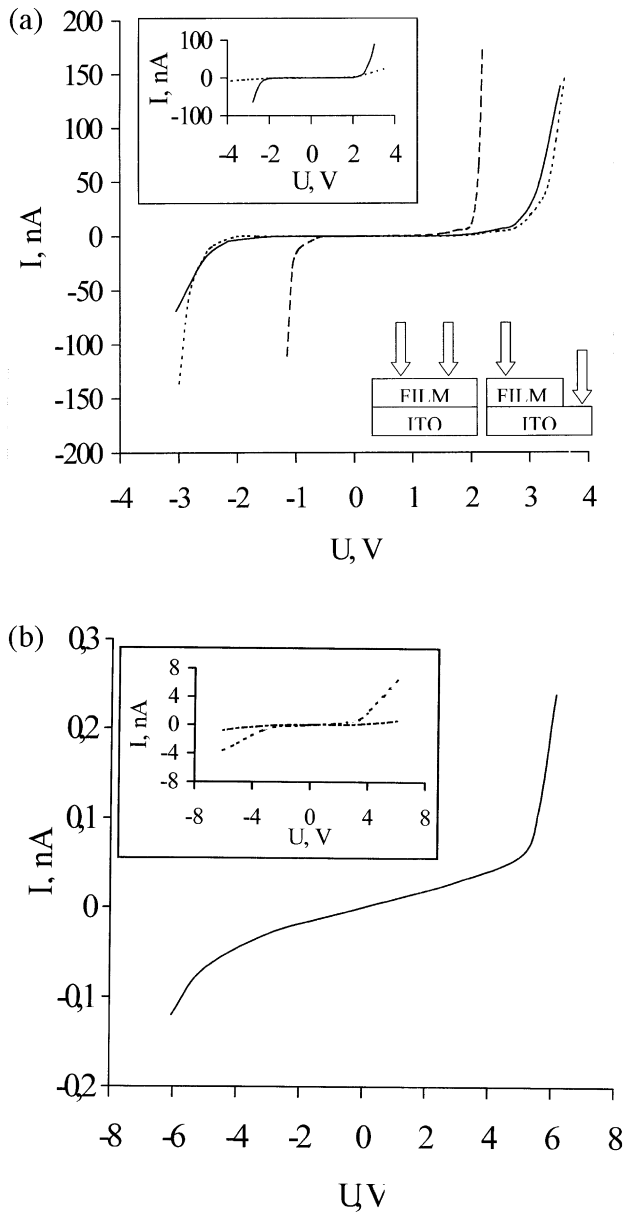

Fig. 4. *I–V* curves for $(TiO_2/PAN)_9TiO_2$ films deposited on ITO-coated glass (a) and porous Si (b). (a) *I–V* curves were measured for transport along the film (solid line) and across the film (dashed and dotted lines) using Pt probes (solid and dotted lines) and Cu probes (dashed line). Inset at the top shows *I–V* curves measured with Pt probes for TiO_2 film that was prepared by dripping the starting TiO_2 solution on ITO-coated glass and drying at ambient temperature: solid line, transport across the film; dotted line, transport along the film. Inset at the bottom shows electrodes positions for current along the film (left) and across the film (right). (b) *I–V* curves were measured for transport along the film using Pt probes. The curves shown in the inset are related to TiO_2 (dotted line) and PAN (solid line) films that were prepared by dripping the starting solutions on porous Si and drying at ambient temperature.

cle agglomerates, which have a lateral extent of about 25 × 40 nm, and separate TiO_2 particles. The vertical size of single particles that is observed as grey-black contrast at their edges experimentally determined as 4–5 nm depending on lateral particle dimensions. The agglomerate consists of several tens of blocks of different shape, whose lateral dimensions range from 5 nm to 7 nm and whose height ranges from 7 nm to 9 nm (observed as white-grey-black contrast).

Thus the TiO_2 layer deposited in one adsorption cycle onto the NH_2-terminal Si surface is formed from separate particle agglomerates or islands of film consisting of the particle agglomerates, while the first TiO_2 layer deposited onto Al_2O_3/Al substrate completely covers the surface and consists of single particles and particle agglomerates. The height of the agglomerates falls within 4–13 nm, corresponding to the TiO_2 particle size in the starting solution, as determined by TEM, and does not assume the particles' aggregation in vertical direction.

3.3. Characterization of the TiO_2/polymer multilayers

The self-assembly of $(TiO_2/polymer)_4TiO_2$ films on glass and $Si(NH_2)$ was monitored by absorption spectroscopic and ellipsometric measurements, respectively. The observed good linearity in the plots of both film thickness (Fig. 3) and absorbance (inset in Fig. 3) versus the number of the TiO_2/polymer adsorption cycles indicates the uniformity of the sandwich units that were self-assembled. However, the average increment in layer thickness is 3.2 nm per PAH/TiO_2 layer (Fig. 3(1)) which is less than TiO_2 particle size (4–13 nm). The thickness of the film deposited in five adsorption cycles is 16 nm, which corresponds to approximately 2–3 TiO_2/PAH layers. When water of pH 2 is used in the rinsing procedure during the film preparation, the thickness of $(TiO_2/PAH)_3TiO_2$ film deposited in four adsorption cycles is 6.7 nm, which equals the average size of TiO_2 particles, and the average increment in the layer thickness is 1.55 nm per PAH/TiO_2 layer (Fig. 3(2)).

AFM image of the $Si(NH_2)/(TiO_2/PAH)_4TiO_2$ sample surface (Fig. 1d) reveals patchy film consisting of islands 100–150 nm wide and up to 23 nm high. Comparing these data with the average film thickness measured by ellipsometry (16 nm), one can conclude that film growth occurs in both lateral and vertical directions. Surface coverage was estimated at about 90%. This is consistent with the model proposed by Kleinfeld and Ferguson for multilayer growth on islands, which eventually coalesce into smoother films [17] .

AFM image (not shown) of the $Si(NH_2)/(TiO_2/PAH)_3TiO_2$ sample, whose preparation involved rinsing with water of pH 2, show a more uniform layer than that prepared by rinsing with water. This fact and the average film thickness measured by ellipsometry (6.7 nm) allow us to conclude that in this case, three adsorption cycles following the first one result in building up the first layer in a lateral direction. Surface coverage was estimated at about 95%.

AFM image (not shown) of the $Al/Al_2O_3/(TiO_2/PEI)_4TiO_2$ film reveals the formation of a well-packed layer. Distinct columns with rather domed tops and the

lack of voids between the columns determine the morphology of the surface. The diameter of the columns ranges from 50 nm to 120 nm. The average roughness of the surface is 21.3 nm.

Thus the quality of the first adsorbed TiO_2 layer is the governing factor in multilayer film growth. Poor surface coverage in the first layer on NH_2-terminated Si surface gives rise to a patchy film grown on islands, while almost 100% coverage in the first layer on the Al_2O_3 surface allows growth of the well-packed multilayer TiO_2/PEI film.

AFM image (not shown) of the $Al/Al_2O_3/(TiO_2/PEI)_4TiO_2$ film heated at 300°C for 30 min reveals no cracks on the film surface. The columns became thinner (diameter 10–60 nm) and their tops are rather tapered. This allows us to conclude that the heat treatment causes compaction of the TiO_2 nanoparticles in the columns. It should be noted that the fast decomposition of polyethylenimine (mol. wt. 13 000) was not observed at 300°C. The average roughness of the film surface is 26.2 nm. Thermal analysis (QD-1500, Hungary) of the starting xerogel has shown 20.3% weight loss between 150°C and 300°C. The exothermic peaks at 173°C and 285°C in DTA are due to the elimination of coordinated water molecules and the decomposition of organic residue, respectively. One can suppose that the same processes occur during the heat-treatment of the $(TiO_2/PEI)_4TiO_2$ film, which can result in compaction of the TiO_2 nanoparticle aggregates.

3.4. Electrical measurements

Typical *I–V* curves with transport along (M/film/M)) (where M is Pt or Cu probe) and across (M/film/ITO/M), the multilayer $(TiO_2/PAN)_9TiO_2$ films deposited on conducting (ITO-coated glass) and non-conducting (porous Si, $R > 10^{11}$ O) substrates are presented in Fig. 4a,b. In all cases, the *I–V* curves show rectifying behaviour of the heterostructures. (a preliminary experiment has shown ohmic *I–V* characteristic for M/ITO/M structure.) The resistivity of the heterostructures calculated for the low-current region is about 10^{10} Ω. The values of the energetic barriers in $Pt/(TiO_2/PAN)_9TiO_2/Pt$ and $Pt/(TiO_2/PAN)_9TiO_2/ITO/Pt$ structures are estimated as 6 eV and 4 eV, respectively. These values are more than those in structures $Pt/TiO_2/Pt$ (~3.5 eV), Pt/PAN/Pt (~45 eV), and $Pt/TiO_2/ITO/Pt$ (3.5 eV) (see insets at the top of Fig.4 a,b) that allow to assume a contribution of theTiO_2/PAN barrier. The values of the energetic barriers in both $Cu/(TiO_2/PAN)_9TiO_2/Cu$ and $Cu/(TiO_2/PAN)_9TiO_2/ITO/Cu$ structures are estimated as 2.1 eV. One can suppose that the rectifying behaviour of the structures under investigation is determined by properties of the M/film contact with transport via electronic states in the energetic band of heterojunction structure.

4. Conclusions

AFM, STM and ellipsometric study of the layer-by-layer self-assembly of TiO_2/polymer composite films has shown that the quality of the first adsorbed TiO_2 layer is the governing factor in multilayer film growth. Poor surface coverage in the first layer gives rise to film growth on islands. The first layer has been found to consist of single particles and particle agglomerates 30–120 nm wide. The surface coverage in the layer is determined by the chemical composition of the substrate surface and water pH in post-adsorption rinsing procedure. Well-packed TiO_2/polymer film completely covering the surface has been prepared in five adsorption cycles on Al_2O_3/Al substrate. The film remained crack-free after heat treatment at 300°C. *I–V* curve measurement reveals high resistivity ($R \sim 10^{10}$ O in the voltage range from −2 V to +3 V) of TiO_2/polymer films prepared in ten adsorption cycles. The thermal and electrical properties of the films make them promising for application as insulating layers in low-voltage electronic devices.

Acknowledgements

This work has been supported in part by Civilian Research and Development Foundation, USA, grant UC1-338. Digital Instruments Nanoscope IIIa was provided by National Science Foundation, USA, grant CHE-9626326.

References

[1] B. O'Regan, J. Moser, M. Anderson, M. Gratzel, J. Phys. Chem. 94 (1990) 8720.
[2] M. Gratzel, MRS Bull. October (1993) 61.
[3] D. Liu, P.V. Kamat, J. Phys. Chem. 97 (1993) 10769.
[4] R. Vogel, K. Pohl, H. Weller, Chem. Phys. Lett. 174 (1990) 241.
[5] C.J. Brinker, G.W. Scherer, Sol-Gel Science. The Physics and Chemistry of Sol-Gel Processing, Academic Press, New York, 1990.
[6] K. Yeng, Y. Lam, Thin Solid Films 109 (1983) 169.
[7] A. Ennaoui, S. Fiechter, H. Tributsch, M. Giersig, R. Vogel, H. Weller, J. Electrochem. Soc. 139 (1992) 2514.
[8] S. Kurtz, R. Gordon, Thin Solid Films 147 (1987) 167.
[9] Y.-C. Shen, et al., Thin Solid Films 257 (1995) 144.
[10] F. Grant, Rev. Mod. Phys. 31 (1959) 636.
[11] M. Litter, J. Navio, J. Photochem. Photobiol. A: Chem. 98 (1996) 171.
[12] J.M. Marshall, N. Kirov, A. Vavrec, Electronic, Optoelectronic and Magnetic Thin Films, Wiley, New York, 1994.
[13] J.H. Fendler, F.C. Meldrum, Adv. Mater. 7 (1995) 607.
[14] N. Kotov, I. Dekany, J. Fendler, J. Phys. Chem. 99 (1995) 13065.
[15] J.H. Cheung, A.F. Fou, M.F. Rubner, Thin Solid Films 244 (1994) 985.
[16] A.Yu. Borovikov, L.V. Levash, A.A. Marchenko, A.G. Naumovets, et al., Izvestia RAS Ser.Phys. 41 (1996) 6.
[17] E.R. Kleinfeld, G.R. Ferguson, Chem. Mater. 8 (1997) 1575.